Special classes of iron(II) azole spin crossover compounds

Koningsbruggen, Petra J. van

Link to publication in University of Groningen/UMCG research database

Special Classes of Iron(II)
Azole Spin Crossover Compounds

Petra J. van Koningsbruggen

Stratingh Institute of Chemistry and Chemical Engineering, University of Groningen,
Nijenborgh 4, 9747 AG, Groningen, The Netherlands
P.van.Koningsbruggen@chem.rug.nl

Abstract In this chapter, selected results obtained so far on Fe(II) spin crossover compounds of 1,2,4-triazole, isoxazole and tetrazole derivatives are summarized and analysed. These materials include the only compounds known to have Fe(II)N$_6$ spin crossover chromophores consisting of six chemically identical heterocyclic ligands. Particular attention is paid to the coordination modes for substituted 1,2,4-triazole derivatives towards Fe(II) resulting in polynuclear and mononuclear compounds exhibiting Fe(II) spin transitions. Furthermore, the physical properties of mononuclear Fe(II) isoxazole and 1-alkyl-tetrazole compounds are discussed in relation to their structures. It will also be shown that the use of α,β- and α,ω-bis(tetrazol-1-yl)alkane type ligands allowed a novel strategy towards obtaining polynuclear Fe(II) spin crossover materials.

Keywords Spin crossover · Fe(II) · 1,2,4-Triazole · Isoxazole · Tetrazole

Abbreviations

4-R-trz	4-substituted-1,2,4-triazole
Htrz	1,2,4–4H-triazole
trz	1,2,4-triazolato
hyetrz	4-(2′-hydroxy-ethyl)-1,2,4-triazole
NH$_2$trz	4-amino-1,2,4-triazole

Hpt   3-(pyridin-2-yl)-1,2,4-triazole
H3mpt   3-methyl-5-(pyridin-2-yl)-1,2,4-triazole
abpt   4-amino-3,5-bis(pyridin-2-yl)-1,2,4-triazole
TCNQ   7,7′,8,8′-tetracyanoquinodimethane
phen   1,10-phenanthroline
mbpt   4-p-methylphenyl-3,5-bis(pyridin-2-yl)-1,2,4-triazole
mmbpt   4-m-methylphenyl-3,5-bis(pyridin-2-yl)-1,2,4-triazole
btzp   1,2-bis(tetrazol-1-yl)propane
btze   1,2-bis(tetrazol-1-yl)ethane
btzb   1,4-bis(tetrazol-1-yl)butane
LIESST   light-induced excited spin-state trapping

1
Introduction

Over the past few decades, a large variety of ligand systems have been tested with the aim of obtaining novel iron(II) spin crossover systems which could possibly be utilised in electronic devices [1]. In most cases an Fe(II)N$_6$ chromophore is required in order to generate the spin crossover phenomenon [2]. A large majority of the ligands used are represented by heterocyclic systems, in which the lone electron pair on the nitrogen atom coordinates to the Fe(II) ion.

Only for 4-R-substituted 1,2,4-triazoles, isoxazoles and 1-alkyl-tetrazoles (Fig. 1), has the Fe(II)N$_6$ spin crossover chromophore been found to consist of six chemically identical heterocyclic ligands. These spin transition materials are of particular interest. Since only a single N-donor ligand is involved in the synthetic procedure, the formation of mixed ligand species is avoided, and hence rather high yields are usually obtained. In addition, the choice of such relatively small heterocyclic ligands favours almost regular O$_h$ symmetry about the Fe(II) ion. This is especially so for low-spin Fe(II).

In this chapter, selected results obtained so far on Fe(II) spin crossover compounds of these ligand systems are compiled and analysed.
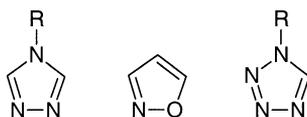

Fig. 1 4-R-1,2,4-Triazole, isoxazole and 1-alkyl-tetrazole

2
Fe(II) Spin Crossover Compounds of 1,2,4-Triazoles

2.1
Coordination Properties of 1,2,4-Triazole Derivatives

The 1,2,4-triazole system has been found to be particularly suited towards generating spin crossover behaviour in Fe(II)N$_6$ derivatives of the simple molecule and in bidentate and tridentate systems containing at least one 1,2,4-triazole ring. The ambidentate nature of the 1,2,4-triazole ring is closely associated with tautomerism of the 1,2,4-triazole nucleus, as shown in Fig. 2.

The N-1 coordination mode has been found in bidimensional- [3] and in tridimensional materials [4] derived from 4,4′-bis-1,2,4-triazole, as well as in mononuclear compounds of bidentate 1,2,4-triazole ligands in which the N-4 atom is protected from coordination by a non-coordinating substituent, as in 4-amino-3,5-bis(pyridin-2-yl)-1,2,4-triazole [5–8], 4-*p*-methylphenyl-3,5-bis(pyridin-2-yl)-1,2,4-triazole [9] and 4-*m*-methylphenyl-3,5-bis(pyridin-2-yl)-1,2,4-triazole [9].

The N-4 coordination towards Fe(II) has been found in mononuclear Fe(II) spin crossover compounds containing bidentate 1,2,4-triazole ligands [10–13], as well as tridentate ligands bearing no substituent at N-4 of the 1,2,4-triazole ring [14–16]. The only exception known is the mononuclear Fe(II) spin crossover compound of the tridentate hydrotris(1,2,4-triazol-1-yl)borate [17–21], where coordination is through N-1 rather than N-4. This probably occurs because of the resulting favourable geometry of the chelate rings.

The N-2, N-4 bridging coordination mode has not (yet) been observed in Fe(II) spin crossover compounds, whereas the N-1, N-2 bridging mode has been confirmed by X-ray structure determinations of oligomeric and polymeric Fe(II) spin crossover materials. Depending on the nature of the substituted 1,2,4-triazole ligand and the presence of potentially coordinating an-
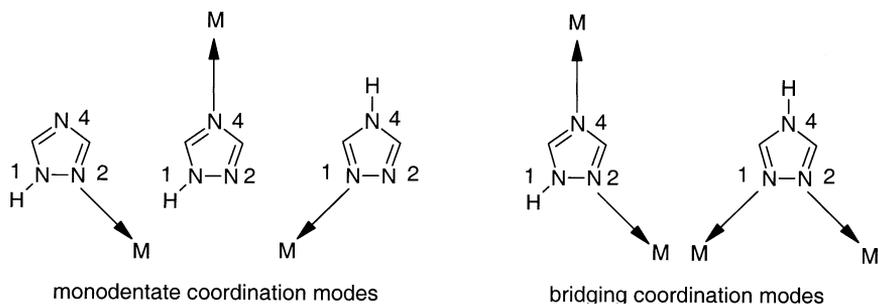

monodentate coordination modes   bridging coordination modes

Fig. 2 Possible coordination modes of 1H(4H)-1,2,4-triazole

ions and/or solvent molecules, the spin crossover materials may be dinuclear [22], linear trinuclear [23] or linear polynuclear [24–54]. Only in the linear trinuclear [23] and linear polynuclear [24–54] materials does the 1,2,4-triazole molecule form FeN_6 spin crossover chromophores.

In the following section, attention is directed towards these linear polynuclear Fe(II) spin crossover systems, whereas subsequent sections focus on mononuclear Fe(II) spin transition compounds containing chelating 1,2,4-triazole derivatives.

2.2
Linear Polynuclear Fe(II) Spin Crossover Compounds

Among all Fe(II) spin crossover compounds known to date, the extensively studied polymeric [Fe(4-R-1,2,4-triazole)$_3$](anion)$_2$ systems (R=amino, alkyl, hydroxyalkyl) appear to have the greatest potential for technological applications, for example in molecular electronics [1, 24, 25] or as temperature sensors [24, 26]. This arises because of their near-ideal spin crossover characteristics: pronounced thermochromism, transition temperatures near room temperature, and large thermal hysteresis [1, 24, 27].

Typically, Fe(II) compounds of 4-R-1,2,4-triazole appear as fine microcrystalline powders. Therefore, EXAFS has been the only method available to directly probe the local structure around the metal ion. In addition, the detailed analysis of the multiple scattering EXAFS signal displayed at the double metal-metal distance has confirmed metal alignment in these compounds [28, 29]. In fact, for [Fe(Htrz)$_2$(trz)](BF$_4$) and [Fe(Htrz)$_3$](BF$_4$)$_2$.H$_2$O (Htrz=1,2,4–4H-triazole; trz=1,2,4-triazolato) EXAFS studies pointed out that the compounds consist of linear chains with typical Fe–Fe separations of 3.65 Å in the low-spin state [28]. Later, the EXAFS data for these Fe(II) derivatives were compared with those of the structurally characterised Cu(II) derivative [Cu(hyetrz)$_3$](ClO$_4$)$_2$.3H$_2$O (hyetrz=4-(2′-hydroxy-ethyl)-1,2,4-triazole), confirming that both metal ions form one-dimensional polymeric systems [30]. The structure of [Cu(hyetrz)$_3$](ClO$_4$)$_2$.3H$_2$O (Fig. 3) shows Cu(II) ions linked by triple N-1,N-2 1,2,4-triazole bridges yielding a chain with alternating Cu1–Cu2 and Cu2–Cu3 distances of 3.853(2) Å and 3.829(2) Å, respectively. It is important to note that even though the Cu(II) coordination sphere is Jahn-Teller distorted, the chain shows only a relatively small deviation from linearity.

The spin crossover characteristics of the corresponding Fe(II) compounds may be fine tuned by the systematic variation of the substituent at N-4 of the 1,2,4-triazole ring, as well as by changing the non-coordinated anionic groups. In this way, thermochromic Fe(II) materials showing a spin transition close to room temperature and accompanied by hysteresis have been obtained. As an example, the optical reflectivity measurements record-
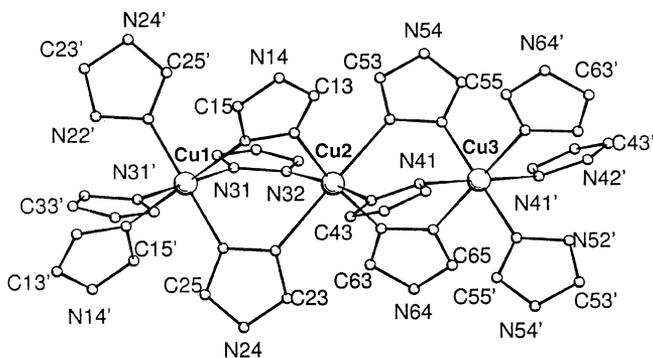
Fig. 3 Projection showing the structure of [Cu(4-(2'-hydroxy-ethyl)-1,2,4-triazole)$_3$] (ClO$_4$)$_2$.3H$_2$O at 298 K (reprinted with permission from [30]. Copyright (1997) American Chemical Society)

ed for [Fe(NH$_2$trz)$_3$](2-naphthalene sulfonate)$_2$.xH$_2$O (x=0, 2; NH$_2$trz=4-amino-1,2,4-triazole) are shown in Fig. 4 [31].

At room temperature, the thermodynamically stable state for [Fe(NH$_2$trz)$_3$] (2-naphthalene sulfonate)$_2$.2H$_2$O is low-spin. This stabilisation of the low-spin state by interactions with lattice water molecules has frequently been observed for mononuclear Fe(II) spin crossover compounds [15, 55–57]. Upon heating, the compound loses its lattice water with an accompanying abrupt change from low-spin to high-spin. When the dehydrated material is cooled, an abrupt high-spin to low-spin transition occurs at $T_{1/2}\downarrow$=283 K. Subsequent reheating reveals a hysteresis loop of 14 K centred close to room temperature (290 K).

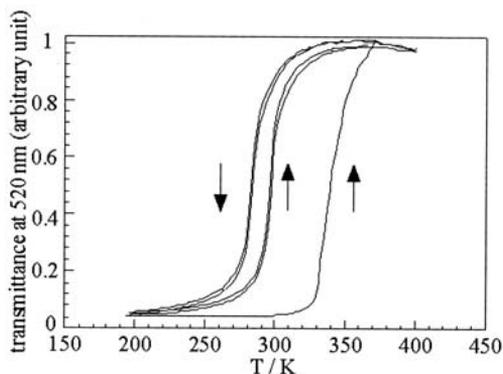**Fig. 4** Optical reflectivity measurement (intensity vs temperature; recorded at 1 K min^{-1}) for [Fe(4-amino-1,2,4-triazole)$_3$](2-naphthalene sulfonate)$_2$.xH$_2$O (x=0, 2) ([31] (reproduced with permission of the Royal Society of Chemistry)

Non-solvated [Fe(NH$_2$trz)$_3$](2-naphthalene sulfonate)$_2$ [31] represents one of the very few Fe(II) spin crossover materials showing a spin transition with hysteresis and an associated thermochromic effect near room temperature. A further example is [Fe(NH$_2$trz)$_3$](tosylate)$_2$,which has been reported to have a hysteresis loop of width 17 K around 290 K [32]. Moreover, by forming the mixed-ligand species [Fe(Htrz)$_{3-3x}$(NH$_2$trz)$_{3x}$](ClO$_4$)$_2$.nH$_2$O thermal hysteresis ($\Delta T_{1/2}$=17 K) centred around 304 K has also been obtained [33]. The examples do not seem to be restricted to 4-amino-1,2,4-triazole: in addition, the spin transition in [Fe(hyetrz)$_3$]I$_2$ (hyetrz=4-(2′-hydroxy-ethyl)-1,2,4-triazole) is associated with thermal hysteresis ($\Delta T_{1/2}$= 12 K) centred around 291 K [34].

2.3
Mononuclear Fe(II) Spin Crossover Compounds of Tridentate Chelating 1,2,4-Triazole Derivatives

Spin transitions occurring above room temperature have also been observed for mononuclear compounds. The bis[hydrotris(pyrazol-1-yl)borate]iron(II) system [58] has been known for more than thirty years and this also displays a spin transition above room temperature (G.J. Long, F. Grandjean, D.L. Reger, this volume). The related system bis[hydrotris(1,2,4-triazol-1-yl)borate]iron(II), [Fe{HB(C$_2$H$_2$N$_3$)$_3$}$_2$], has been studied more recently [17–21]. This is the only mononuclear Fe(II) spin transition compound containing six N-1-donating 1,2,4-triazole nuclei. The anionic tridente ligand is shown in Fig. 5.

[Fe{HB(C$_2$H$_2$N$_3$)$_3$}$_2$] has been obtained by dehydration under heating of the low-spin hexahydrate. The crystal structure for this hexahydrate has been determined at room temperature [17]. It clearly contains Fe(II) ions in the low-spin state (average Fe–N distance=1.99 Å). The dehydrated derivative [Fe{HB(C$_2$H$_2$N$_3$)$_3$}$_2$] has been reported to exhibit a very abrupt spin transition between 334–345 K via variable temperature UV-vis and [57]Fe Mössbauer spectroscopy studies [19]. After the publication of a preliminary magnetic study in 1994 [19], a more detailed report appeared in 1998 [20].
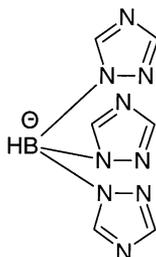

Fig. 5 The hydrotris(1,2,4-triazol-1-yl)borate anion

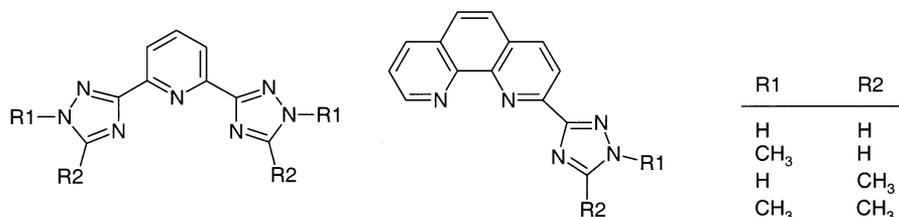| R1	R2
H	H
CH$_3$	H
H	CH$_3$
CH$_3$	CH$_3$

Fig. 6 2,6-Bis(triazol-3-yl)pyridine, 2-triazolyl-1,10-phenanthroline, and their methyl-substituted derivatives

The coordination properties of two other classes of tridentate chelating 1,2,4-triazole-containing-ligands have been studied by Goodwin et al. [14–16]. These are represented by 2,6-bis(triazol-3-yl)pyridine [14] and 2-triazolyl-1,10-phenanthroline [15, 16] and their methyl-substituted derivatives (H. A. Goodwin, this volume) (Fig. 6).

The crystal structures of [Fe(2,6-bis(triazol-3-yl)pyridine)$_2$](NO$_3$)$_2$.4H$_2$O and [Ni(2,6-bis(triazol-3-yl)pyridine)$_2$]Cl$_2$.3H$_2$O revealed that the tridentate ligand coordinates to the metal(II) ion using both N-4 atoms of the two 1,2,4-triazole moieties together with the pyridyl nitrogen atom [14]. The N-1 of the 1,2,4-triazole ring that is not coordinated sets up an important hydrogen-bonding network involving the anions and the non-coordinated water molecules. It was found that the water content had a strong influence on the spin state of Fe(II). [Fe(2,6-bis(triazol-3-yl)pyridine)$_2$]Cl$_2$.3H$_2$O is high-spin at room temperature and exhibits a partial transition to low-spin upon cooling. Upon heating the material above 100 °C, the water is lost and the anhydrous species is low-spin. It is worth noting that the removal of solvent molecules leads in this case to the exact opposite effect to that observed in the linear chain compounds of formula [Fe(4-R-1,2,4-triazole)$_3$](anion)$_2$.xH$_2$O [27, 31, 34, 36], where the dehydration upon heating is accompanied by an Fe(II) spin transition from the low-spin to the high-spin state. On the other hand, Fe(II) compounds of 2,6-bis(triazol-3-yl)pyridine ligands bearing *N*-methyl substituents yielded Fe(II) systems, which could only be obtained as non-hydrated materials, in which the [FeN$_6$]$^{2+}$ derivative is high-spin.

Structure determinations of several Fe(II) compounds of 2-triazolyl-1,10-phenanthroline and its methyl-substituted derivatives proved that in addition to the two nitrogen donor atoms of the 1,10-phenanthroline entity, the N-4 of the 1,2,4-triazole ring participates in coordination, even when a methyl substituent occupies the position adjacent to this donor atom [15, 16]. All compounds obtained exhibit Fe(II) spin crossover behaviour, its extent depending on the nature of the anionic groups and the solvent content.

2.4
Mononuclear Fe(II) Spin Crossover Compounds of Bidentate Chelating 1,2,4-Triazole Derivatives

Using bidentate chelating 1,2,4-triazole-based ligands, various families of Fe(II) spin crossover systems have been obtained. Among these, the mononuclear Fe(II) spin crossover compounds of 3-(pyridin-2-yl)-1,2,4-triazole derivatives have been known for several years [10–12]. Early studies on $[Fe(Hpt)_3](anion)_2.(solvent)_x$ (Hpt=3-(pyridin-2-yl)-1,2,4-triazole (Fig. 7); anion=Cl^-, ClO_4^-, PF_6^-, BF_4^-; solvent=C_2H_5OH, H_2O) and $[Fe(H3mpt)_3](anion)_2.(H_2O)_x$ (H3mpt=3-methyl-5-(pyridin-2-yl)-1,2,4-triazole; anion=ClO_4^-, PF_6^-) have been reported by Stupik et al. [10, 11] and Sugiyarto et al. [12].

In the absence of any x-ray crystallographic data, the early results could not be explained satisfactorily. It has been assumed that the Fe(II) ion is in a six-nitrogen environment of three bidentate 3-(pyridin-2-yl)-1,2,4-triazole ligands coordinating via the 1,2,4-triazole-N-4 and the pyridine-N atoms. The asymmetry encountered in the bidentate ligand may lead to the formation of FeL$_3$ units of *facial* or *meridional* geometry. Moreover, the spin transition characteristics appeared to be dependent on the amount and nature of the incorporated solvent molecules [10–12]. In addition, two different iron(II) high-spin sites have been detected in the hydrated BF_4^- and ClO_4^- Fe(II) tris(3-(pyridin-2-yl)-1,2,4-triazole) compounds [10–12]. More recent work, including the x-ray crystal structure of $[Fe(Hpt)_3](BF_4)_2.2H_2O$ [13], has clarified some of these points.

$[Fe(Hpt)_3](BF_4)_2.2H_2O$ shows gradual and incomplete spin crossover behaviour with $T_{1/2}$=135 K [13]. The crystal structure determination carried out at 95 and 250 K revealed only one crystallographically independent $[Fe(Hpt)_3]^{2+}$ cation with the *mer* configuration, despite the observation of two high-spin Fe(II) doublets in the ^{57}Fe Mössbauer spectra. The Fe(II) is octahedrally surrounded by three bidentate Hpt ligands coordinating through the N of the pyridine ring and N-4 of the 1,2,4-triazole moiety. The average Fe–N bond length is reduced by about 0.15 Å at 95 K. As expected, the N–Fe–N4 bite angles increase with decreasing temperature, ranging from 75.53–77.13° at 250 K to 80.17–80.86° at 95 K. Therefore, the octahedron about the Fe(II) ion becomes more regular upon the transition from the high-spin to the low-spin state. However, a large deviation from the ideal value of 90° remains, which is due to the expected restriction of the Hpt bite angle within
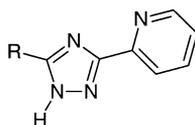

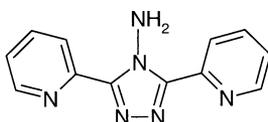**Fig. 7** 3-(Pyridin-2-yl)-1,2,4-triazole (Hpt)

Fig. 8 4-Amino-3,5-bis(pyridin-2-yl)-1,2,4-triazole (abpt)

the five-membered chelate ring, as well as the fact that at 95 K about 35% of the Fe(II) ions remain high-spin.

It has been postulated that the origin of the two different high-spin Fe(II) doublets observed in the ^{57}Fe Mössbauer spectra may be that a small fraction (about 6%) of the Fe(II) ions experience a different local environment, most likely in the distribution of the non-coordinating solvent and anion molecules, from that of the majority of the high-spin Fe(II) ions.

In the second family of spin crossover compounds containing bidentate 1,2,4-triazole-based ligands, additional N-donating co-anions occupy *trans* positions about the Fe(II) ion. The first representative of this family is [Fe(abpt)$_2$(TCNQ)$_2$] (abpt=4-amino-3,5-bis(pyridin-2-yl)-1,2,4-triazole (Fig. 8), TCNQ=7,7′,8,8′-tetracyanoquinodimethane), which is the only Fe(II) complex containing coordinated radical anions. It undergoes a complete, gradual spin crossover ($T_{1/2}$=280 K) [5]. This compound represents one of the few cases in which the Fe(II) spin crossover centre contains two monodentate substituents in *trans* positions. This geometry has now been found for several bis(thiocyanato)iron(II) spin crossover compounds [3b, 7, 9, 59, 60]. The first was observed more than a decade ago for [Fe(4,4′-bis-1,2,4-triazole)$_2$(NCX)$_2$] (X=S [3a, 3b], or Se [3c]), which consists of layers of six-coordinated Fe(II) ions linked in the equatorial plane by single bridges of the 4,4′-bis-1,2,4-triazole ligand via the N-1 atoms. Recently, the dicyanamide anion has also been shown to lead to *trans* [Fe(abpt)$_2$(N(CN)$_2$)$_2$] entities, which is also a spin crossover system [8].

The structure of [Fe(abpt)$_2$(TCNQ)$_2$] was determined at 298 and 100 K. The molecular structure is depicted in Fig. 9.

The unit-cell contains one [Fe(abpt)$_2$(TCNQ)$_2$] unit with Fe(II) at the inversion centre. The coordination sphere in the equatorial plane is formed by two bidentate abpt ligands coordinating via N(pyridyl) and N-1(1,2,4-triazole). The high-spin to low-spin change is accompanied by a non-uniform shortening of the Fe–N bond lengths. The Fe–N(pyridyl) distance is 2.12(1) Å at 298 K and 2.02(1) Å at 100 K, whereas the Fe–N-1(1,2,4-triazole) distance is 2.08(1) Å at 298 K and 2.00(2) Å at 100 K. More significant changes in the Fe–N(TCNQ) bond lengths are observed: 2.16(1) Å at 298 K and 1.93(1) Å at 100 K, the latter distance being particularly short. This change of 0.23 Å is among the largest that has been observed for Fe(II) spin crossover compounds. It can probably be related to the extended π-system of TCNQ and the increased $d_\pi \rightarrow \pi^\star$ backbonding when Fe(II) is in the low-
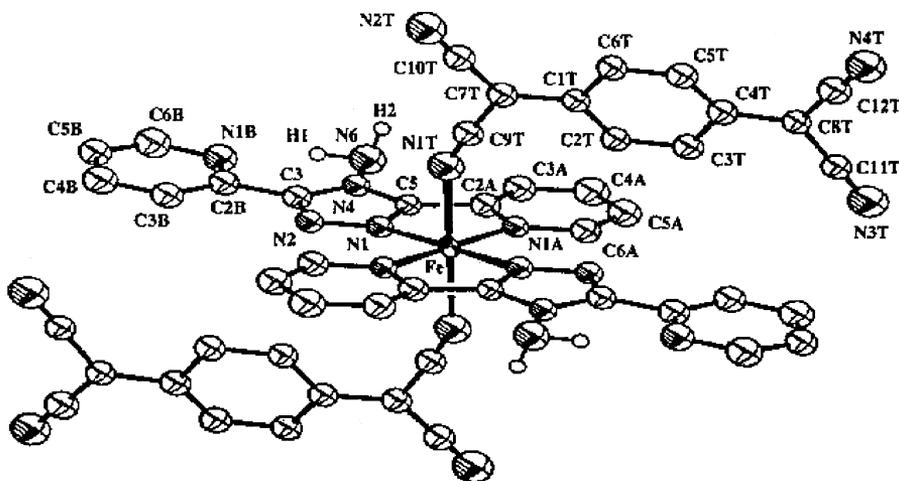
Fig. 9 Projection showing the structure of [Fe(abpt)$_2$(TCNQ)$_2$] at 298 K (reprinted with permission from [5]. Copyright (1996) American Chemical Society)

spin state. The [Fe(abpt)$_2$(TCNQ)$_2$] entities are packed in such a way that π-stacking of the TCNQ radical anions results in the formation of (TCNQ)$_2^{2-}$ diads in the usual eclipsed conformation (Fig. 10) [61].

The presence of these (TCNQ)$_2^{2-}$ diads also explains the magnetic data, which indicate only a complete, gradual spin crossover with $T_{1/2}$=280 K [5]. Since the antiferromagnetic coupling within such a stacked entity is very strong, these form diamagnetic units over the whole temperature range studied, and hence do not contribute to the magnetism. In addition, the interplanar distances between two symmetry related TCNQ radical anions originating from two nearest neighbour [Fe(abpt)$_2$(TCNQ)$_2$] units are within the range normally encountered for such dimeric (TCNQ)$_2^{2-}$entities. This spacing shortens from 3.22 Å at 298 K to 3.15 Å at 100 K with the change from high-spin to low-spin. The *trans* arrangement of the TCNQ radical anions is feasible in this instance because of the reduced repulsive forces between the hydrogen atoms of the coordinated diimines, compared to those in [Fe(phen)$_2$(NCS)$_2$] (phen=1,10-phenanthroline) and related systems which have the *cis* configuration. This *trans* geometry in [Fe(abpt)$_2$(TCNQ)$_2$] is further stabilised by stacking of the radical anions together with hydrogen bond formation between the amino group of abpt and the cyano nitrogen atom of the TCNQ radical anion.

This compound is not only of note because its spin crossover is centered near room temperature; the TCNQ radical anions are also directly coordinated to the divalent metal center. In fact, TCNQ has strong electron affinity due to the electron-withdrawing capacity of the four cyano groups, hence TCNQ readily takes on an electron to form the radical anion TCNQ$^{\cdot-}$. Coor-
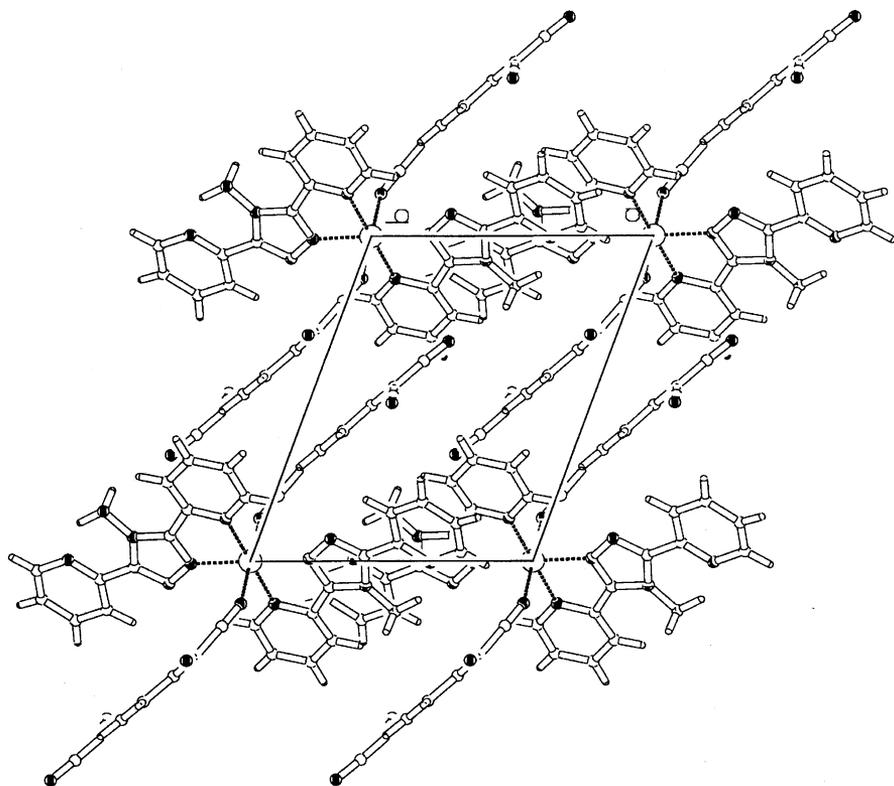
Fig. 10 Projection showing the crystal packing of [Fe(abpt)$_2$(TCNQ)$_2$]

dination to monovalent metal ions has in several cases been observed, however, binding to divalent metal ions very rarely occurs. Besides of its strong electron accepting properties, the poor coordinating power of TCNQ can also be related to crystal packing efficiency considerations – in other words TCNQ entities favour the formation of stacks, and coordination has been found to occur only if the molecules can form at least stacked dimers at the same time.

These structural features observed for [Fe(abpt)$_2$(TCNQ)$_2$] involving pronounced and extended π-π stacking interactions lead to a duality with respect to its gradual spin crossover behaviour. It has generally been accepted that extended π-π interactions may lead to the occurrence of thermal hysteresis in mononuclear Fe(II) spin crossover compounds [62–65]. Clearly, the requirements responsible for cooperative Fe(II) spin crossover behaviour are not easy to define, since obviously [Fe(abpt)$_2$(TCNQ)$_2$] represents an exception to this rule: in spite of the pronounced TCNQ π-π stacking interactions, the Fe(II) spin crossover displays at best weak cooperativity.
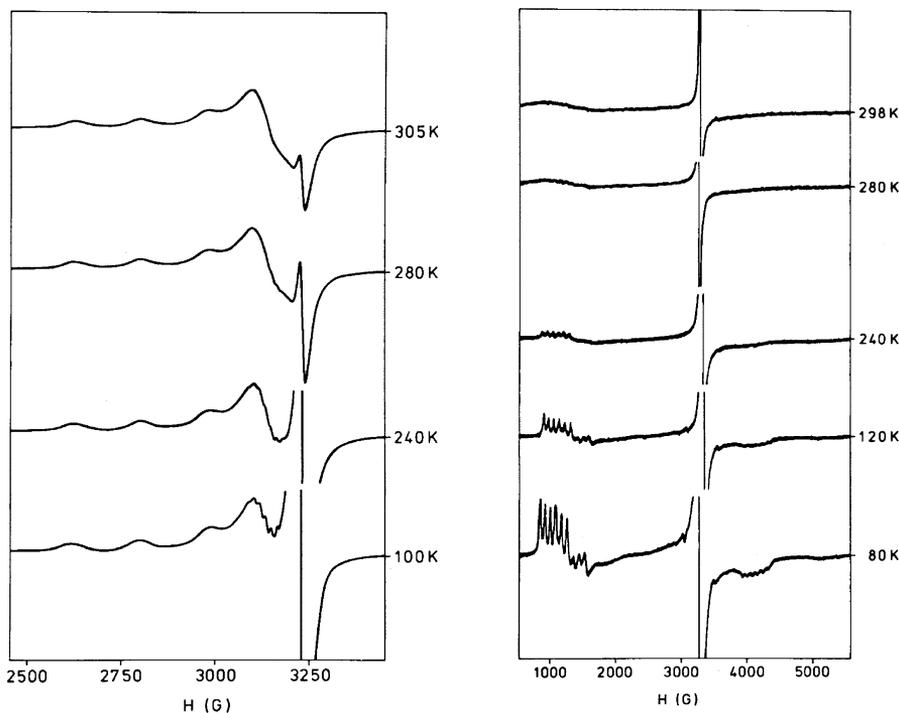
Fig. 11 Selected X-band powder ESR spectra of Cu(II)- (left) and Mn(II)-doped (right) [Fe(abpt)$_2$(TCNQ)$_2$] (reprinted with permission from [5]. Copyright (1996) American Chemical Society)

The spin transition in [Fe(abpt)$_2$(TCNQ)$_2$] can be monitored by focusing on the changes in the ν_{CN} stretching vibrations in the variable temperature FT-IR spectra [5]. The various cyano absorptions show characteristic frequencies and changing intensities upon the Fe(II) spin crossover, which also allows the direct observation of the coexistence of low-spin and high-spin Fe(II) species within the Fe(II) spin crossover temperature range. Related investigations have been carried out for other spin transition systems. In these cases, changes in far infrared Fe–N(ligand) vibrations [66, 67], or M–NCX (X=S, Se) ν_{CN} stretching vibrations [68–70] have generally been studied as a function of the temperature.

The spin transition could be monitored by ESR in Mn(II) or Cu(II)-doped materials. The related pure compounds of the dopants are strictly isomorphous with [Fe(abpt)$_2$(TCNQ)$_2$]. The inclusion of a small percentage of the paramagnetic Mn(II) or Cu(II) ions provides ESR probes for monitoring the Fe(II) spin transition from within the crystal lattice. The results are displayed in Fig. 11.

Although the TCNQ radical anions form diamagnetic diads, the narrow signal at g=2.00, indicative of TCNQ$^{\cdot-}$ impurities, remains visible in all spectra. The Fe(II) host lattice is paramagnetic above the transition temperature and essentially diamagnetic below this temperature. Above $T_{1/2}$, the ESR spectra are poorly resolved due to exchange broadening, but this changes dramatically after the spin transition, and spectra with sharp and distinct features typical for the dopant in a tetragonal environment are observed. The Cu(II)-doped Fe(II) species shows a broad signal with $g_\perp$=2.09 and $g_{//}$=2.25, together with hyperfine structure ($A_{//}$=180 Gauss) above $T_{1/2}$, whereas at $T_{1/2}$ and below, superhyperfine structure ($A_{N//}$=16 Gauss) appears. The superhyperfine structure splits each line into nine components, due to the coupling of the unpaired electron situated on the Cu(II) ion with the four abpt nitrogen atoms located in the equatorial coordination sphere. For the Mn(II)-doped material, a very broad signal at g=2.00 is visible above $T_{1/2}$, which sharpens at $T_{1/2}$ to reveal zero-field splitting yielding signals at g=1.6 and g=5.5. Six hyperfine lines ($A_{//}$=80 Gauss) are clearly visible on both signals.

Further studies have shown that instead of TCNQ$^{\cdot-}$, NCS$^-$ or NCSe$^-$ [6,7] can also occupy the *trans*-located axial positions, resulting in spin crossover compounds with structures comparable to those of [Fe(abpt)$_2$(TCNQ)$_2$] [5]. The Fe(II) spin transition is also gradual for these derivatives, however, with considerably lower transition temperatures: 224 K for the NCSe$^-$ derivative and 180 K for the NCS$^-$ analogue.

Recently, the crystal structure of the related [Fe(abpt)$_2$(N(CN)$_2$)$_2$] has been determined [8]. The species undergoes an incomplete transition ($T_{1/2}$= approximately 86 K) with an indication of two steps, the origin of which is unclear. Below 60 K, about 37% of the Fe(II) ions remain high-spin.

[FeL$_2$(NCS)$_2$] compounds have also been recently reported with 4-*p*-methylphenyl-3,5-bis(pyridin-2-yl)-1,2,4-triazole (mbpt) and 4-*m*-methylphenyl-3,5-bis(pyridin-2-yl)-1,2,4-triazole (mmbpt) (Fig. 12) [9]. For both compounds the structure has been determined at 293 K.

The ligand mbpt coordinates to Fe(II) through the N of the pyridyl substituent (Fe–N=2.213(3) Å) and N-1 of the 1,2,4-triazole ring (Fe–N1= 2.192(2) Å). Two N-donating thiocyanate anions occupy *trans* positions at significantly shorter distances (Fe–N=2.114(3) Å). These distances are consistent with high-spin Fe(II). The spin transition ($T_{1/2}$=231 K) in this instance is more abrupt than in [Fe(abpt)$_2$(anion)$_2$] (anion=TCNQ$^-$ [5], NCS$^-$ [6, 7], NCSe$^-$ [6, 7], [N(CN)$_2$]$^-$ [8]). This may be related to the replacement of the 4-amino substituent in abpt by the 4-*p*-methylphenyl substituent in mbpt, resulting in more pronounced π-π stacking interactions, which may enhance the cooperativity of the spin crossover.

In contrast, in [Fe(mmbpt)$_2$(NCS)$_2$], the two thiocyanate anions are coordinated in *cis* positions at relatively short distances (Fe–N=2.051(3) Å). The bidentate ligands coordinate at much longer distances (Fe–
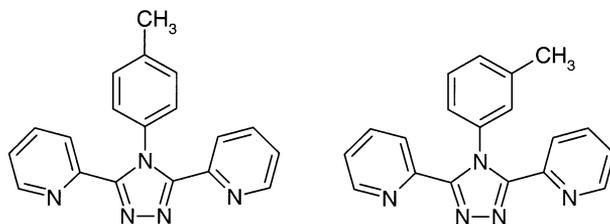
Fig. 12 4-*p*-Methylphenyl-3,5-bis(pyridin-2-yl)-1,2,4-triazole (mbpt) and 4-*m*-methylphe-nyl-3,5-bis(pyridin-2-yl)-1,2,4-triazole (mmbpt)

N(pyridyl)=2.217(2) Å and Fe–N-1(1,2,4-triazole)=2.248(3) Å). [Fe(mmbpt)$_2$(NCS)$_2$] is high-spin down to 77 K.

3
Fe(II) Spin Crossover Compounds of Isoxazoles

In 1977 Driessen and van der Voort identified an extremely abrupt spin crossover with $T_{1/2}$ of 213 K for [Fe(isoxazole)$_6$](ClO$_4$)$_2$ [71]. Although various spectroscopic techniques have been employed to study this spin transition, the structural features of this compound at the time could not be determined, due to its extreme sensitivity to decomposition [71]. The same applies to the tetrafluoroborate salt that also displays a spin crossover, but in this instance a two-step transition was observed [71].

Fig. 13 Temperature dependence of μ_{eff} both in the cooling and warming modes for [Fe(isoxazole)$_6$](BF$_4$)$_2$ ([72] – reproduced with permission of the Royal Society of Chemistry)

Fig. 14 Projection showing the structure of [Fe(isoxazole)$_6$](BF$_4$)$_2$ ([72] – reproduced with permission of the Royal Society of Chemistry)

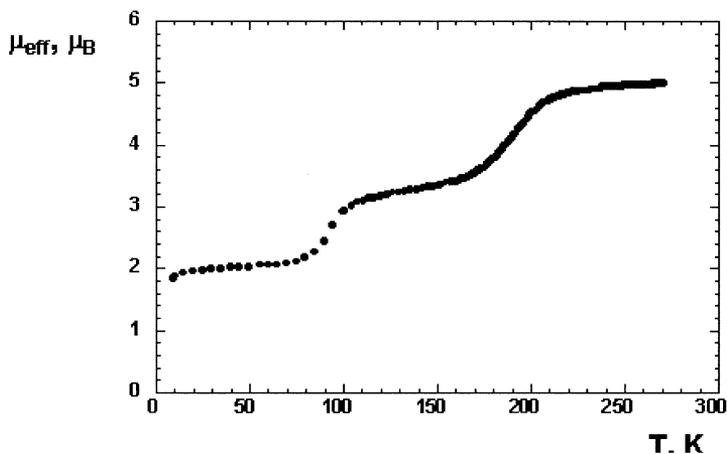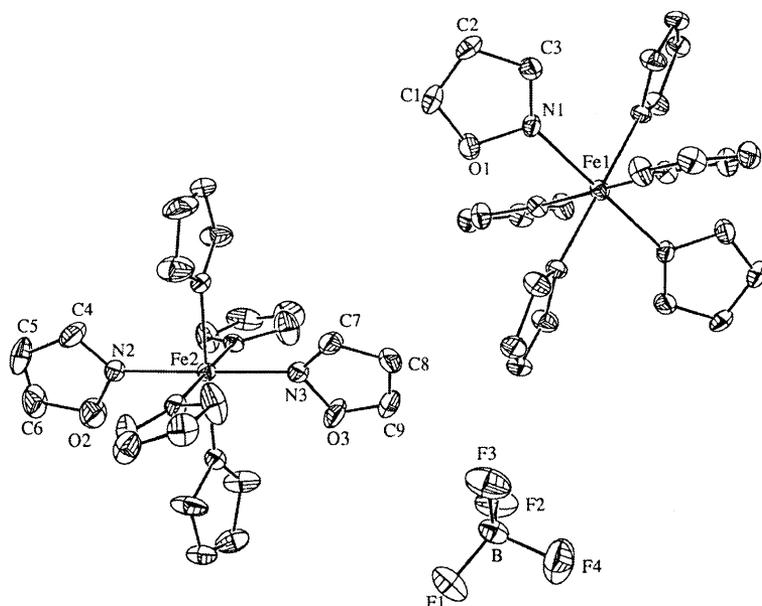Recently, this family of isoxazole compounds has been re-examined with particular emphasis on the tetrafluoroborate salt. These studies included the first extended magnetic and structural characterisation of [Fe(isoxazole)$_6$](BF$_4$)$_2$ [72]. In addition, the double salt [Fe(isoxazole)$_6$][Fe(isoxazole)$_4$(H$_2$O)$_2$](BF$_4$)$_4$ was isolated [73].

The initially reported magnetism for [Fe(isoxazole)$_6$](BF$_4$)$_2$ was reproduced (Fig. 13) and the two-step nature of the spin transition was found to arise from two crystallographically independent [Fe(isoxazole)$_6$]$^{2+}$ sites [72]. These sites, designated Fe1 and Fe2, are present in the ratio 1:2 in the high-spin structure determined at 230 K (See Fig. 14). The distinct spin crossover behaviour of each Fe(II) site could be related to the inequality of the Fe1 and Fe2 chromophores, such as the slight differences in bond lengths and bond angles, as well as in the geometrical disposition (in other words the dihedral angles between neighbouring isoxazole ligands). Analysis of the magnetic data revealed that the transition occurring at 91 K could be attributed to Fe1, whereas the transition taking place at 192 K was due to Fe2.

A further report dealt with the synthesis, variable temperature magnetic susceptibility measurements, and crystal structure determination at various temperatures (115, 136, 140, 150 and 231 K; space group *P*-1) of [Fe(isoxazole)$_6$][Fe(isoxazole)$_4$(H$_2$O)$_2$](BF$_4$)$_4$ [73]. The molecular structure of this well-defined double salt consists of two mononuclear Fe(II) dications,
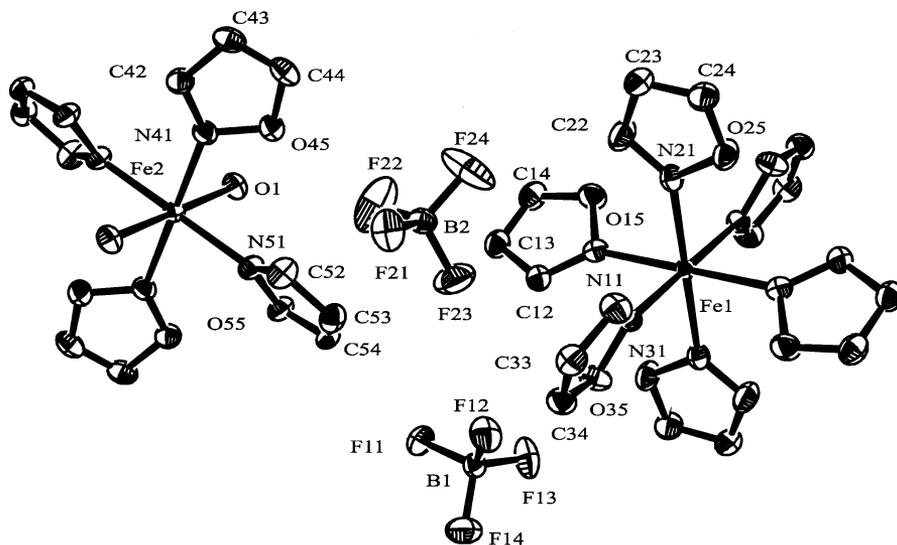
Fig. 15 Projection showing the structure of $[Fe(isoxazole)_6][Fe(isoxazole)_4(H_2O)_2](BF_4)_4$ at 140 K [73]

$[Fe(isoxazole)_6]^{2+}$ and $[Fe(isoxazole)_4(H_2O)_2]^{2+}$, together with four non-co-ordinated tetrafluoroborate anions (Fig. 15). The structural details for the low-field *trans* $[Fe(isoxazole)_4(H_2O)_2]^{2+}$ are consistent with a high-spin Fe(II) chromophore (average Fe–O=2.09 Å and Fe–N=2.19 Å), whereas those for $[Fe(isoxazole)_6]^{2+}$ show a marked temperature dependence (average Fe–N=1.98 Å at 115 K and 2.17 Å at 231 K) related to the reversible low-spin to high-spin transition. From magnetic susceptibility measurements, the transition temperature has been found to be $T_{1/2}$=137 K.

4
Fe(II) Spin Crossover Compounds of Tetrazoles

4.1
Mononuclear Fe(II) Spin Crossover Compounds

The mononuclear hexakis(1-alkyl-tetrazole)iron(II) compounds with various anions have been extensively studied. It appears that the spin crossover characteristics of compounds with different alkyl substituents attached to N-1 of the tetrazole heavily depend on the crystal structure features. The transitions may be abrupt or rather gradual, complete or only involving a fraction of the Fe(II) ions, and the $T_{1/2}$ values lie in the range 63–204 K [2c, 2f, 2g, 74–81]. Interest in these systems has focused on their suitability for detailed studies of the LIESST effect (A. Hauser, this volume).

Recently, tetrazole ligands with halogen containing substituents have been added to this family. The first member is [Fe(1-(2-chloroethyl)tetrazole)$_6$](BF$_4$)$_2$ [82], whose crystal structure shows two symmetry-equivalent Fe(II) ions in the high-spin state at room temperature. On the other hand, the magnetic susceptibility data indicate that two spin transitions in the ratio 1:1 take place at 190 K and 107.5 K. This seems to be inconsistent with the structural data, but they may have their origin in a phase transition taking place at lower temperatures leading to the existence of different Fe(II) sites, or may be the result of additional thermodynamic stability of the mixture of close to 50% of high-spin and 50% of low-spin Fe(II) ions at temperatures between the two steps of the spin crossover.

Among the mononuclear hexakis(1-alkyl-tetrazole)iron(II) compounds, the extensively-studied [Fe(1-propyl-tetrazole)$_6$](BF$_4$)$_2$ [2c, 2f, 2g, 74–78] shows an abrupt spin transition in both cooling and heating mode, a feature which may very well be described by the model of elastic interactions [83]. In addition, an associated hysteresis loop, which is due to a first order crystallographic phase transition, is observed [84]. Since for the envisaged use of Fe(II) spin crossover materials in most feasible technical applications molecular bistability is a necessary criterion, the occurrence of thermal hysteresis is a pre-requisite. Therefore, it is important to acquire a detailed understanding of the factors likely to be responsible for this feature. It appears that the occurrence of thermal hysteresis in mononuclear Fe(II) spin crossover compounds may also be brought about by strong intermolecular interactions resulting from the presence of an important hydrogen-bonding network [85, 86] or extended π-π interactions [62–65].

4.2
Polynuclear Fe(II) Spin Crossover Compounds

The observation of thermal hysteresis associated with the spin transition in particular mononuclear systems described above suggested that a useful strategy for the enhancement of this cooperativity would be the coordination of bi-functional ligand systems leading to polymeric derivatives. This use of ligands capable of linking the active spin-switching metal centres has been motivated by the proposal that efficient propagation of the molecular distortions originating from the Fe(II) spin transition through the crystal lattice would be enhanced by the covalent bonds linking the spin crossover centres.

α,β- and α,ω-bis(tetrazol-1-yl)alkane type ligands were used to obtain polynuclear Fe(II) spin crossover materials. In this section, the compounds that have been reported with the ligands 1,2-bis(tetrazol-1-yl)propane (abbreviated as btzp), 1,2-bis(tetrazol-1-yl)ethane (abbreviated as btze) and 1,4-bis(tetrazol-1-yl)butane (abbreviated as btzb) (Fig. 16) will be discussed.
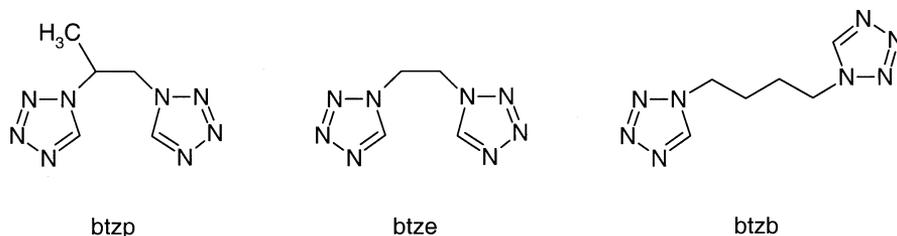
Fig. 16 1,2-Bis(tetrazol-1-yl)propane (btzp), 1,2-bis(tetrazol-1-yl)ethane (btze) and 1,4-bis(tetrazol-1-yl)butane (btzb)

Interest in $[Fe(btzp)_3](ClO_4)_2$ [87] and $[Fe(btze)_3](BF_4)_2$ [88] arises because they represent the first structurally characterised Fe(II) linear chain compounds exhibiting spin crossover. The incomplete transitions are gradual with $T_{1/2}$ of 148 K and 140 K, respectively.

Both compounds crystallise in the trigonal space group $P\bar{3}c1$, and this space group remains unchanged upon the Fe(II) spin crossover. The structure of $[Fe(btzp)_3](ClO_4)_2$ [87] has been solved at 200 K and 100 K, whereas the structure of $[Fe(btze)_3](BF_4)_2$ [88] has been determined at 296, 200, 150 and 100 K. A projection of the linear chain structure of $[Fe(btzp)_3](ClO_4)_2$ [87] is displayed in Fig. 17.

Because of symmetry considerations, in both compounds the Fe(II) ion lies on the threefold axis and has an inversion centre. It is in an octahedral environment formed by six crystallographically related N-4 coordinating 1-tetrazole moieties. The almost perfect O_h symmetry for the FeN_6 core is therefore present in the high-spin and low-spin state. Three bis(tetrazole)alkane ligands, in a bent *syn* conformation, link the Fe(II) centres to form reg-
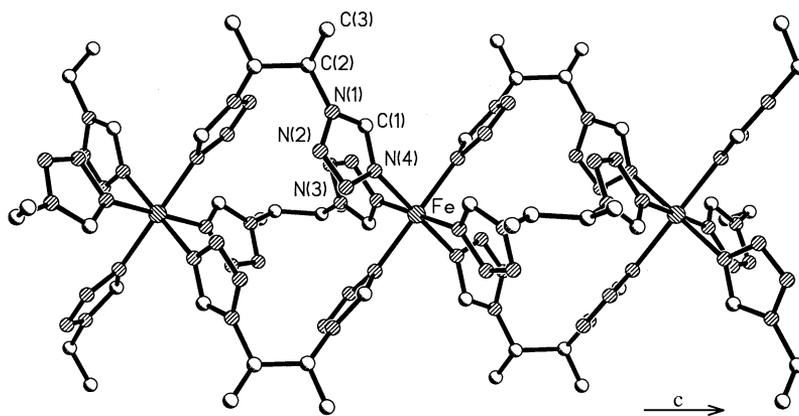

Fig. 17 Projection showing the structure of $[Fe(btzp)_3](ClO_4)_2$ perpendicular to the *c*-axis at 100 K (adapted from [87])

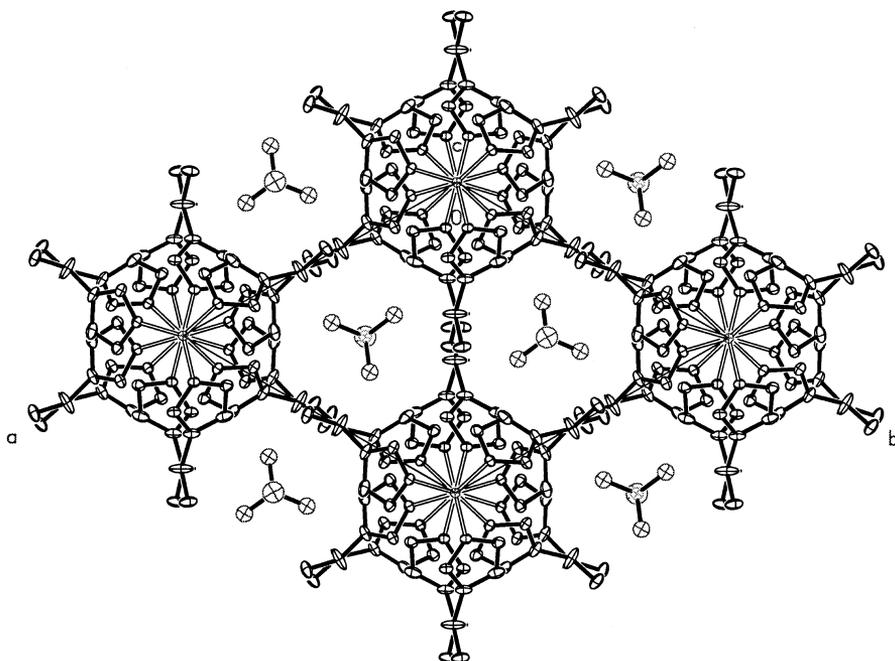**Fig. 18** Projection showing the structure of $[Fe(btzp)_3](ClO_4)_2$ down the *c*-axis at 100 K (adapted from [87])

ular cationic chains running parallel to the crystallographic *c*-axis. The spin crossover is associated with the typical marked temperature dependence of the Fe–N distances, and is also reflected by the Fe–Fe separations over the bis(tetrazole)alkane ligands. The Fe–Fe separations for the btzp ligand are 7.422(1) Å at 200 K and 7.273(1) Å at 100 K, whereas these are 7.477, 7.461, 7.376 and 7.293 Å at 296, 200, 150 and 100 K, respectively, for the btze analogue. In the *ab* plane the linear chains are arranged in a hexagonal close-packed fashion, creating channel-like hexagonal cavities between them, in which the non-coordinated anionic groups are located (Fig. 18).

The gradual spin transition observed for these compounds may be directly related to their structures. It is generally believed that the direct connectivity of the Fe(II) sites in polynuclear Fe(II) spin transition compounds may have a favourable effect on the strength of the elastic interactions between the active Fe(II) spin crossover centres, thereby increasing the cooperativity of the spin transition, leading to very abrupt spin crossover behaviour or even thermal hysteresis. This is illustrated by the properties of the linear chain derivatives of 1,2,4-triazole discussed in Sect. 2.2. When the ligand spacer linking the Fe(II) ions becomes more flexible, as is the case for $[Fe(1,2-bis(tetrazol-1-yl)propane)_3](ClO_4)_2$ [87] and $[Fe(1,2-bis(tetrazol-1-yl)ethane)_3](ClO_4)_2$ [88], the spin crossover behaviour becomes more gradu-
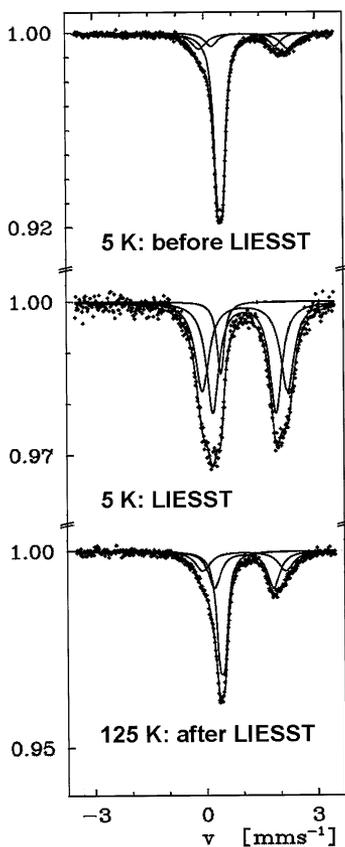
Fig. 19 LIESST effect observed by ^{57}Fe Mössbauer spectroscopy for [Fe(btzp)$_3$](ClO$_4$)$_2$: at 5 K, without light irradiation (top); at 5 K, after light irradiation (middle); at 125 K, after light irradiation (bottom). (Reprinted with permission from [87]. Copyright (2000) American Chemical Society)

al indicating only weak elastic interactions, most probably due to the 1,2-propane or 1,2-ethylene unit acting as some kind of shock absorber and thereby disrupting the communication of the structural changes at the metal centres.

Most interestingly, [Fe(btzp)$_3$](ClO$_4$)$_2$ is the first one-dimensional Fe(II) spin crossover compound, which shows the LIESST effect, detected in this instance by ^{57}Fe Mössbauer spectroscopy (Fig. 19).

At 5 K, the spectrum is dominated (area fraction of 80%) by a singlet, typical for one of the rare cases of cubic local symmetry for low-spin Fe(II). In addition, two distinct high-spin Fe(II) doublets are observed, contributing 16 and 4%, respectively. The presence of two high-spin Fe(II) doublets together with the fact that the Mössbauer resonance lines arising from the

Fig. 20 Projection showing the tentative 3-D model for $[Fe(btzb)_3](ClO_4)_2$ at 150 K ([89] – reproduced with permission of the Royal Society of Chemistry)

high-spin states as well as those from the low-spin state all are broadened, may be related to the disorder encountered in the 1,2-propane linkage, leading to a statistical distribution of different Fe(I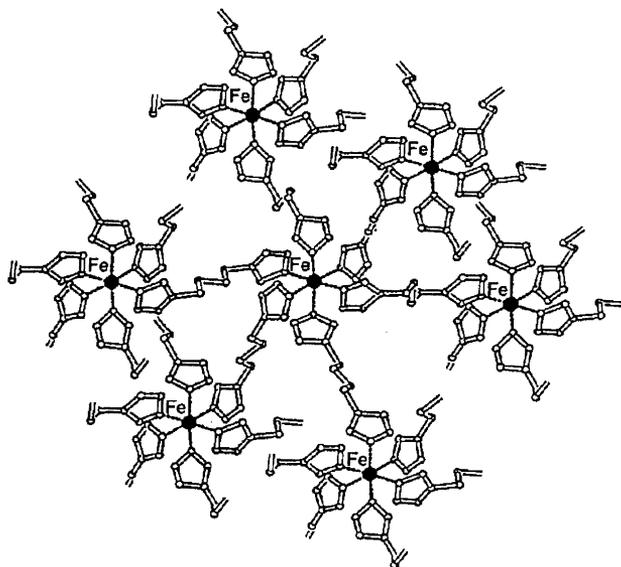I) sites. The second spectrum was recorded after the sample had been irradiated at 5 K with green light using an Argon-ion laser (514 nm, 25 mW cm^{-2}) for 20 minutes. This spectrum shows that the spectral contribution for low-spin Fe(II) has been reduced to 9%, whereas both high-spin fractions have considerably increased to 44% and 47%, respectively. Upon warming the sample up to 20 K, 60% of the high-spin sites were found to have relaxed to the low-spin state. Above 50 K, the relaxation is complete. The ^{57}Fe Mössbauer spectrum recorded at 125 K after LIESST (Fig. 19) is exactly identical to the spectrum recorded upon thermal treatment at the same temperature.

Increasing the length of the alkyl spacer in such a way as to yield 1,4-bis(tetrazol-1-yl)butane (abbreviated as btzb) (Fig. 16), changes the dimensionality of the Fe(II) spin crossover material [89]. In fact, $[Fe(btzb)_3]$ $(ClO_4)_2$ is the first highly thermochromic Fe(II) spin crossover material with a supramolecular catenane structure consisting of three interlocked 3-D networks [89]. Unfortunately, only a tentative model of the 3-D structure of $[Fe(btzb)_3](ClO_4)_2$ could be determined based on the x-ray data collected at 150 K (Fig. 20).

Since each of the btzb ligands is located on an inversion centre, all central C–C linkages are in the *anti* conformation. Of the six independent N–C–C–C

torsions in the ligands, four are also in the *anti* conformation, but two fit the electron density best when brought into a *gauche* conformation. A detailed re-analysis of the crystallographic data has been carried out recently [90]. This revealed a structure showing three symmetry related, interpenetrating, 3-D Fe-btzb networks. The shortest Fe–Fe separations of 8.3 and 9.1 Å occur between Fe(II) ions of two unconnected networks. The crystal structure of the Cu(II) analogue confirmed this threefold interpenetrating 3-D catenane structure [91]. Interestingly, the crystal structure determination did not reveal any well-defined specific intra- or intermolecular interactions, which could be responsible for the stabilisation of this unusual supramolecular structure. It may well be that the driving force for the formation of these remarkable supramolecular 3-D catenane materials lies in the conformation adopted by the alkyl spacer used to link the tetrazole moieties. Upon increasing the spacer length, the *anti* conformation, as has been found for the free btzb and for the Fe(II) catenane of btzb [89], is favoured over the bent *syn* conformation as found in the linear chains of ligands with smaller spacers [87, 88, 92].

The system is strongly thermochromic, so variable temperature optical reflectivity measurements could be used to determine the spin crossover characteristics along with the usual magnetic susceptibilty measurements. These revealed that only ca. 16% of the Fe(II) ions participate in the spin transition, characterised by $T_{1/2}\downarrow$=150 K and $T_{1/2}\uparrow$=170 K. This hysteresis loop of width 20 K is reversible over several thermal cycles. It is worth noting that this is the largest thermal hysteresis observed up to now for iron(II) tetrazole derivatives. Apparently, the rigidity originating from the interweaving within this threefold 3-D interlocked supramolecular lattice, is responsible for the efficient propagation of the elastic interactions leading to this type of cooperative spin crossover behaviour. However, the same factors may also be invoked for explaining the small fraction of Fe(II) ions undergoing the spin transition. Most probably, the structural changes accompanying the Fe(II) spin transition modify the structure in such a way that further spin crossover of the high-spin Fe(II) ions upon cooling is severely disfavoured. The small low-spin fraction present at low temperatures can be converted to a metastable high-spin state by irradiation with green light (by the LIESST effect).

5
Conclusions

All the hexakis(ligand) Fe(II) materials derived from isoxazole, 1-alkyl-tetrazole and 4-R-1,2,4-triazole exhibit very favourable Fe(II) spin crossover response functions, which make them the likely compounds of choice for various applications in molecular electronics. The interconversion from low-spin

(S=0) and high-spin (S=2) represents the magnetic response, and moreover, it is associated with a pronounced thermochromic effect. Interestingly, these are among the very few ligand systems known for which the absorption spectrum of the Fe(II) spin transition materials is not obscured by ligand- or charge-transfer bands, conferring the colour arising from the *d-d* transitions of the Fe(II) ion to the compound (purple to pink in the low-spin state and colourless in the high-spin state).

The Fe(II) spin crossover chromophores in compounds of isoxazole and tetrazole all consist of an FeN$_6$ octahedron comprising six chemically identical heterocyclic ligands. Although the isoxazole nucleus has been found to be able to coordinate in a monodentate, as well as in a bidentate bridging fashion through the N and/or O atoms, the predominant coordination mode towards transition metal ions appears to be the monodentate-N mode [93]. It is this which occurs in [Fe(isoxazole)$_6$](BF$_4$)$_2$ [72] and [Fe(isoxa-zole)$_6$][Fe(isoxazole)$_4$(H$_2$O)$_2$](BF$_4$)$_4$ [73]. Therefore, these Fe(II) isoxazole materials show some structural similarity with the mononuclear hexakis(1-alkyl-tetrazole)iron(II) compounds [2c, 2f, 2g, 74–81]. In contrast to this, the [Fe(4-R-1,2,4-triazole)$_6$]$^{2+}$ spin crossover chromophore has almost exclusively been found in polynuclear compounds. Depending on the nature of the substituted 1,2,4-triazole ligand and the presence of potentially co-ordinating water molecules, the spin crossover materials may be linear trinuclear [23], linear polynuclear [24–54] or even tridimensional [4]. The only mononuclear Fe(II) compound containing a hexakis(N1–1,2,4-tria-zole)iron(II) chromophore is bis[hydrotris(1,2,4-triazol-1-yl)borate]iron(II) [17–21].

Although 1,2,4-triazole frequently tends to establish a direct bridge be-tween Fe(II) ions, currently this has not yet been structurally identified for isoxazole and tetrazole. However, the formation of polynuclear Fe(II) spin crossover materials containing tetrazole ligands has been achieved with bi-functional systems in which the coordinating moieties are sufficiently sepa-rated to preclude chelate ring formation. In this respect it is interesting to note that results indicative of the formation of polynuclear Fe(II) spin cross-over materials containing tetrazolate bridges have been available since 1966. At that time, Holm and Donnelly reported their experiments involving 1H-tetrazole and Fe(II) salts [94]. Both cream-yellow and pink products were described suggesting that different spin states were involved. In addition, analytical data indicated the likely presence of bridging tetrazole. Therefore, these systems may resemble the rigid 1,2,4-triazole-bridged species and war-rant further study. Nevertheless, the further exploration of this family of compounds may find its place in a research field focusing on new types of explosives – the materials explode upon heating above 110 °C – rather than in investigations aimed at the development of new Fe(II) spin crossover ma-terials for "safe" applications in molecular electronics.

References

1. a. Kahn O, Kröber J, Jay C (1992) Adv Mater 4:718; b. Jay C, Grolière F, Kahn O, Kröber J (1993) Mol Cryst Liq Cryst 234:255
2. a. Haasnoot JG (1996) In: Kahn O (ed) Magnetism: A Supramolecular Function. Kluwer Academic Publishers, Dordrecht, p 299; b. Haasnoot JG (2000) Coord Chem Rev 200–202:131; c. Gütlich P (1981) Struct Bond (Berlin) 44:83; d. Zarembowitch J, Kahn O (1991) New J Chem 15:181; e. König E (1987) Prog Inorg Chem 35:527; f. Gütlich P, Hauser A, Spiering H (1994) Angew Chem Int Ed Engl 33:2024; g. Gütlich P (1997) Mol Cryst Liq Cryst 305:17
3. a. Vreugdenhil W, Haasnoot JG, Kahn O, Thuéry P, Reedijk J (1987) J Am Chem Soc 109:5272; b. Vreugdenhil W, van Diemen JH, de Graaff RAG, Haasnoot JG, Reedijk J, van der Kraan AM, Kahn O, Zarembowitch J (1990) Polyhedron 9:2971; c. Ozarowski A, Shunzhong Y, McGarvey BR, Mislankar A, Drake JE (1991) Inorg Chem 30:3167
4. Garcia Y, Kahn O, Rabardel L, Chansou B, Salmon L, Tuchagues JP (1999) Inorg Chem 38:4663
5. Kunkeler PJ, van Koningsbruggen PJ, Cornelissen JP, van der Kraan AM, Spek AL, Haasnoot JG, Reedijk J (1996) J Am Chem Soc 118:2190
6. Moliner N, Muñoz MC, van Koningsbruggen PJ, Real JA (1998) Inorg Chim Acta 274:1
7. Moliner N, Muñoz MC, Létard S, Létard J-F, Solans X, Burriel R, Castro M, Kahn O, Real JA (1999) Inorg Chim Acta 291:279
8. Moliner N, Gaspar AB, Muñoz MC, Niel V, Cano J, Real JA (2001) Inorg Chem 40:3986
9. Zhu D, Xu Y, Yu Z, Guo Z, Sang H, Liu T, You X (2002) Chem Mater 14:838
10. Stupik P, Zhang JH, Kwiecien M, Reiff WM, Haasnoot JG, Hage R, Reedijk J (1986) Hyperfine Interact 725
11. Stupik P, Reiff WM, Hage R, Jacobs J, Haasnoot JG, Reedijk J (1988) Hyperfine Interact 343
12. Sugiyarto KH, Craig DC, Rae AD, Goodwin HA (1995) Aust J Chem 48:35
13. Stassen AF, de Vos M, van Koningsbruggen PJ, Renz F, Ensling J, Kooijman H, Spek AL, Haasnoot JG, Gütlich P, Reedijk J (2000) Eur J Inorg Chem 2231
14. Sugiyarto KH, Craig DC, Rae AD, Goodwin HA (1993) Aust J Chem 46:1269
15. Sugiyarto KH, Craig DC, Rae AD, Goodwin HA (1996) Aust J Chem 49:505
16. Sugiyarto KH, Craig DC, Goodwin HA (1996) Aust J Chem 49:497
17. Janiak C (1994) J Chem Soc Chem Commun 545
18. Janiak C (1994) Chem Ber 127:1379
19. Janiak C, Scharmann TG, Green JC, Parkin RPG, Kolm MJ, Riedel E, Mickler W, Elguero J, Claramunt RM, Sanz D (1996) Chem Eur J 2:992
20. Janiak C, Scharmann TG, Bräuniger T, Holubová J, Nádvorník M (1998) Z Anorg Allg Chem 624:769
21. van Koningsbruggen PJ, Miller JS (unpublished results)

22. Kolnaar JJA, de Heer MI, Kooijman H, Spek AL, Schmitt G, Ksenofontov V, Gütlich P, Haasnoot JG, Reedijk J (1999) Eur J Inorg Chem 881
23. a. Vos G, Le Fêbre RA, de Graaff RAG, Haasnoot JG, Reedijk J (1983) J Am Chem Soc 105:1682; b. Vos G, de Graaff RAG, Haasnoot JG, van der Kraan AM, de Vaal P, Reedijk J (1984) Inorg Chem 23:2905; c. Kolnaar JJA, van Dijk G, Kooijman H, Spek AL, Ksenofontov V, Gütlich P, Haasnoot JG, Reedijk J (1997) Inorg Chem 36:2433; d. Thomann M, Kahn O, Guilhem J, Varret F (1994) Inorg Chem 33:6029
24. Kahn O, Martinez-Jay C (1998) Science 279:44
25. Kahn O (1993) Molecular Magnetism. VCH Publishers, New York, p 53
26. Garcia Y, van Koningsbruggen PJ, Codjovi E, Lapouyade R, Kahn O, Rabardel L (1997) J Mater Chem 7:857
27. Kahn O, Codjovi E, Garcia Y, van Koningsbruggen PJ, Lapouyade R, Sommier L (1996) Molecule-Based Magnetic Materials. In: Turnbull MM, Sugimoto T, Thompson LK (eds) Symposium Series No. 644, American Chemical Society, Washington, DC, p 298
28. Michalowicz A, Moscovici J, Ducourant B, Cracco D, Kahn O (1995) Chem Mater 7:1833
29. Michalowicz A, Moscovici J, Kahn O (1997) J Phys IV France 7:633
30. Garcia Y, van Koningsbruggen PJ, Bravic G, Guionneau P, Chasseau D, Cascarano GC, Moscovici J, Lambert K, Michalowicz A, Kahn O (1997) Inorg Chem 36:6357
31. van Koningsbruggen PJ, Garcia Y, Codjovi E, Lapouyade R, Kahn O, Fournès L, Rabardel L (1997) J Mater Chem 7:2069
32. Codjovi E, Sommier L, Kahn O, Jay C (1996) New J Chem 20:503
33. Kröber J, Codjovi E, Kahn O, Grolière F, Jay C (1993) J Am Chem Soc 115:9810
34. Garcia Y, van Koningsbruggen PJ, Lapouyade R, Rabardel L, Kahn O, Wieczorek M, Bronisz R, Ciunik Z, Rudolf MF (1998) CR Acad Sci Paris IIC:523
35. Roubeau O, Alcazar Gomez JM, Balskus E, Kolnaar JJA, Haasnoot JG, Reedijk J (2001) New J Chem 25:144
36. Garcia Y, van Koningsbruggen PJ, Lapouyade R, Fournès L, Rabardel L, Kahn O, Ksenofontov V, Levchenko G, Gütlich P (1998) Chem Mater 10:2426
37. Kahn O, Sommier L, Codjovi E (1997) Chem Mater 9:3199
38. Kahn O, Codjovi E (1996) Phil Trans R Soc London A 354:359
39. Lavrenova LG, Ikorskii VN, Varnek VA, Oglezneva IM, Larionov SV (1986) Koord Khim 12:207
40. Lavrenova LG, Ikorskii VN, Varnek VA, Oglezneva IM, Larionov SV (1990) Koord Khim 16:654
41. Lavrenova LG, Ikorskii VN, Varnek VA, Oglezneva IM, Larionov SV (1993) J Struct Chem 34:960
42. Varnek VA, Lavrenova LG (1995) J Struct Chem 36:104
43. Lavrenova LG, Yudina NG, Ikorskii VN, Varnek VA, Oglezneva IM, Larionov SV (1995) Polyhedron 14:1333
44. Érenburg SB, Bausk NV, Varnek VA, Lavrenova LG (1996) J Magn Magn Mater 157–158:595
45. Shvedenkov YG, Ikorskii VN, Lavrenova LG, Drebushchak VA, Yudina NG (1997) J Struct Chem 38:579
46. Varnek VA, Lavrenova LG (1997) J Struct Chem 38:850
47. Erenburg SB, Bausk NV, Lavrenova LG, Varnek VA, Mazalov LN (1997) Solid State Ionics 101–103:571
48. Sugiyarto KH, Goodwin HA (1994) Aust J Chem 47:263
49. Yoshizawa K, Miyajima H, Yamabe T (1997) J Phys Chem B 101:4383

50. Murakami Y, Komatsu T, Kojima N (1999) Synth Met 103:2157
51. Kojima N, Murakami Y, Komatsu T, Yokoyama T (1999) Synth Met 103:2154
52. Toyazaki S, Nakanishi M, Komatsu T, Kojima N, Matsumura D, Yokoyama T (2001) Synth Met 121:1794
53. Takeda S, Ueda T, Watanabe A, Maruta G (2001) Polyhedron 20:1263
54. Smit E, Manoun B, de Waal D (2001) J Raman Spectrosc 32:339
55. Sugiyarto KH, Graig DC, Rae AD, Goodwin HA (1994) Aust J Chem 47:869
56. Sugiyarto KH, Goodwin HA (1988) Aust J Chem 41:1645
57. Sorai M, Ensling J, Hasselbach KM, Gütlich P (1977) Chem Phys 20:197
58. a. Jesson JP, Trofimenko S, Eaton DR J (1967) Am Chem Soc 83:3158; b. Hutchinson B, Daniels L, Henderson E, Neill P (1979) Chem Soc Chem Commun 1003; c. Grandjean F, Long GJ, Hutchinson BB, Ohlhausen L, Neill P, Holcomb JD (1989) Inorg Chem 28:4406
59. Real JA, Andréz E, Muñoz MC, Julve M, Granier T, Bousseksou A, Varret F (1995) Science 268:265
60. Roux C, Zarembowitch J, Gallois B, Granier T, Claude R (1994) Inorg Chem 33:2273
61. a. Cornelissen JP, van Diemen JH, Groeneveld LR, Haasnoot JG, Spek AL, Reedijk J (1992) Inorg Chem 31:198; b. Lacroix P, Kahn O, Gleizes A, Valade L, Cassoux P (1984) New J Chem 8:643; c. Miller JS, Zhang JH, Reiff WM, Dixon DA, Preston LD, Reis Jr. AH, Gebert E, Extine M, Troup J, Epstein AJ, Ward MD (1987) J Phys Chem 91:4344; d. Humphrey DG, Fallon GD, Murray KS (1988) J Chem Soc Chem Commun 1356; e. Lau C-P, Singh P, Cline SJ, Seiders R, Brookhart M, Marsh WE, Hodgson DJ, Hatfield WE (1982) Inorg Chem 21:208; f. Kaim W, Moscherosch M (1994) Coord Chem Rev 129:157
62. Letard JF, Guionneau P, Codjovi E, Lavastre O, Bravic G, Chasseau D, Kahn O (1997) J Am Chem Soc 119:10861
63. Letard JF, Guionneau P, Rabardel L, Howard JAK, Goeta AE, Chasseau D, Kahn O (1998) Inorg Chem 37:4432
64. Zhong ZJ, Tao JQ, Yu Z, Dun CY, Liu YJ, You XZ (1998) J Chem Soc Dalton Trans 327
65. Boca R, Boca M, Dlhán L, Falk K, Fuess H, Haase W, Jaroščiak R, Papánková B, Renz F, Vrbová M, Werner R (2001) Inorg Chem 40:3025
66. Hutchinson B, Daniels L, Henderson E, Neill P (1979) J Chem Soc Chem Commun 1003
67. Müller EW, Ensling J, Spiering H, Gütlich P (1983) Inorg Chem 22:2074
68. Baker Jr. WA, Long GJ (1965) J Chem Soc Chem Commun 15:368
69. a. König E, Madeja K (1967) Inorg Chem 6:48; b. König E, Madeja K (1967) Spectrochim Acta A 23:45
70. Zilverentant CL, van Albada GA, Bousseksou A, Haasnoot JG, Reedijk J (2000) Inorg Chim Acta 303:287
71. Driessen WL, van der Voort PH (1977) Inorg Chim Acta 21:217
72. Hibbs W, Arif AM, van Koningsbruggen PJ, Miller JS (1999) Cryst Eng Comm 4
73. van Koningsbruggen PJ, Ksenofontov V, Stauf S, Tremel W, Gütlich P (in preparation, to be submitted to Eur J Inorg Chem)
74. Franke PL, Haasnoot JG, Zuur AP (1982) Inorg Chim Acta. 59:5
75. Müller WE, Ensling J, Spiering H, Gütlich P (1983) Inorg Chem 22:2074
76. Wiehl L (1993) Acta Crystallogr B 49:289
77. Gütlich P, Hauser A (1990) Coord Chem Rev 97:1
78. Gütlich P, Jung J, Goodwin HA (1996) NATO ASI Series, Kluwer Academic, Dordrecht, p 327

79. a. Poganiuch P, Gütlich P (1988) Hyperfine Interact 40:331; b. Adler P, Poganiuch P, Spiering H (1989) Hyperfine Interact 52:47; c. Poganiuch P, Decurtins S, Gütlich P (1990) J Am Chem Soc 112:3270; d. Gütlich P, Poganiuch P (1991) Angew Chem Int Ed Engl 30(8):975; e. Buchen T, Gütlich P (1994) Chem Phys Lett 220:262; f. Hinek R, Spiering H, Schollmeyer D, Gütlich P, Hauser A (1996) Chem Eur J 2:1127; g. Buchen T, Poganiuch P, Gütlich P (1994) J Chem Soc Dalton Trans 2285; h. Jeftic J, Hinek R, Capelli SC, Hauser A (1997) Inorg Chem 36:3080; i. Buchen T, Schollmeyer D, Gütlich P (1996) Inorg Chem 35:155
80. Stassen AF, Roubeau O, Ferrero Gramage I, Linarès J, Varret F, Mutikainen I, Turpeinen U, Haasnoot JG, Reedijk J (2001) Polyhedron 20:1699
81. Roubeau O, Stassen AF, Ferrero Gramage I, Codjovi E, Linarès J, Varret F, Haasnoot JG, Reedijk J (2001) Polyhedron 20:1709
82. Dova E, Stassen AF, Driessen RAJ, Sonneveld E, Goubitz K, Peschar R, Haasnoot JG, Reedijk J, Schenk H (2001) Acta Crystallogr B 57:531
83. a. Sanner I, Meiner E, Köppen H, Spiering H (1984) Chem Phys 86:227; b. Willenbacher N, Spiering H (1988) J Phys C: Solid State Phys 21:1423; c. Spiering H, Willenbacher N (1989) J Phys: Condens Matter 1:10089
84. Jung J, Schmitt G, Wiehl L, Hauser A, Knorr K, Spiering H, Gütlich P (1996) Z Phys B 100:523
85. Sorai M, Ensling J, Hasselbach KM, Gütlich P (1977) Chem Phys 20:197
86. a. Buchen T, Gütlich P, Sugiyarto KH, Goodwin HA (1996) Chem Eur J 2:1134; b. Sugiyarto KH, Weitzner K, Craig DC, Goodwin HA (1997) Aust J Chem 50:869
87. van Koningsbruggen PJ, Garcia Y, Kahn O, Fournès L, Kooijman H, Haasnoot JG, Moscovici J, Provost K, Michalowicz A, Renz F, Gütlich P (2000) Inorg Chem 39:891
88. Schweifer J, Weinberger P, Mereiter K, Boca M, Reichl C, Wiesinger G, Hilscher G, van Koningsbruggen PJ, Kooijman H, Grunert M, Linert W (2002) Inorg Chim Acta 339:297
89. van Koningsbruggen PJ, Garcia Y, Kooijman H, Spek AL, Haasnoot JG, Kahn O, Linares J, Codjovi E, Varret F (2001) J Chem Soc Dalton Trans 466
90. Mereiter K, Kooijman H, van Koningsbruggen PJ, Grunert M, Weinberger P, Linert W (2002, unpublished results)
91. van Koningsbruggen PJ, Bravic G, Chasseau D, Mereiter K, Grunert M, Weinberger P, Linert W (in preparation)
92. van Koningsbruggen PJ, Garcia Y, Bravic G, Chasseau D, Kahn O (2001) Inorg Chim Acta 326:101
93. Munsey MS, Natale NR (1991) Coord Chem Rev 109:251
94. Holm RD, Donnelly PL (1966) J Inorg Nucl Chem 28:1887